

MCMC determination of the cosmic UV background at $z \simeq 0$ from $H\alpha$ fluorescence

Davide Caruso,¹ Francesco Haardt,^{1,2★} Michele Fumagalli^{3,4} and Sebastiano Cantalupo⁵

¹*DiSAT, Università dell’Insubria, Via Valleggio 11, I-22100 Como, Italy*

²*INFN, Sezione di Milano-Bicocca, Piazza delle Scienze 3, I-20123 Milano, Italy*

³*Institute for Computational Cosmology, Durham University, South Road, Durham DH1 3LE, UK*

⁴*Centre for Extragalactic Astronomy, Durham University, South Road, Durham DH1 3LE, UK*

⁵*Department of Physics, ETH Zurich, Wolfgang Pauli Strasse 27, CH-8093 Zurich, Switzerland*

Accepted 2018 October 30. Received 2018 October 29; in original form 2018 August 29

ABSTRACT

In a recent paper we reported on the detection of a diffuse $H\alpha$ glow in the outskirts of the nearby, edge-on disc galaxy UGC 7321 observed with the Multi-Unit Spectroscopic Explorer (MUSE) at the ESO Very Large Telescope. By interpreting the $H\alpha$ emission as fluorescence arising from hydrogen ionized by an external (i.e. extragalactic) radiation field, we estimated the UV background (UVB) intensity in terms of $H\text{I}$ ionization rate (per ion) at $z \simeq 0$ to be in the range $\Gamma_{\text{HI}} \sim 6 - 8 \times 10^{-14} \text{ s}^{-1}$. In the present work, by performing radiative transfer calculations over a large set of models of the gaseous disc of UGC 7321, we refine our estimate and through an MCMC analysis derive a value for the photoionization rate of $\Gamma_{\text{HI}} = 7.27_{-2.90}^{+2.93} \times 10^{-14} \text{ s}^{-1}$. In particular, our analysis demonstrates that this value is robust against large variations in the galaxy model and that the uncertainties are mainly driven by the errors associated with the observed $H\alpha$ surface brightness. Our measurement is consistent with several recent determinations of the same quantity by a completely independent technique (i.e. flux decrement analysis of the $\text{Ly}\alpha$ forest), and support the notion that the low-redshift UVB is largely dominated by active galactic nuclei, possibly with no need of further contribution from star-forming galaxies.

Key words: radiative transfer – methods: numerical – intergalactic medium – cosmology: theory.

1 INTRODUCTION

The reionization of the all-pervading intergalactic medium (IGM), the repository of most of the baryons across the history of the Universe, is a landmark event in the cosmic history of structure formation. Modern observations of the IGM have provided several tests of the Λ CDM paradigm, including a measurement of the power spectrum, upper limits to the neutrino masses, and a measure of baryonic acoustic oscillations (e.g. McDonald et al. 2005; Viel, Haehnelt & Springel 2010; Slosar et al., 2013).

Most of our understanding of IGM physics, and its implication for galaxy formation and metal enrichment, depends critically on the properties of the cosmic ionizing UV background (UVB), the integrated UV emission from all possible emitting sources in the Universe. Massive stars in young star-forming galaxies and accret-

ing supermassive black holes in active galactic nuclei (AGNs) are the most obvious sources of ionizing UV radiation (e.g. Miralda-Escude & Ostriker 1990; Haardt & Madau 1996), still their relative importance across the cosmic time is not firmly established (see e.g. Kulkarni, Worseck & Hennawi 2018, and references therein).

Recent observational and theoretical progress is forging a coherent description of the thermal state and ionization degree of the IGM. The UVB reionized the hydrogen component of the IGM by $z \simeq 6$ (e.g. Davies et al. 2018; Planck Collaboration et al. 2018), while the double reionization of helium occurred later, at $z \gtrsim 3$ (e.g. Worseck et al. 2016), because of the reduced cross-section and higher ionization potential. In the post-reionization Universe, the UVB keeps the bulk of the IGM ionized (e.g. Gunn & Peterson 1965; Bolton & Haehnelt 2007), regulates its temperature (e.g. Theuns et al. 2002), and sets a characteristic mass below which haloes fail to form galaxies (e.g. Okamoto, Gao & Theuns 2008).

In the absence of firm observational constraints on Γ_{HI} the current parametrization of the UVB relies mostly on 1D radiative transfer

* E-mail: haardt@uninsubria.it

(RT) calculations that follow the build-up of the UVB accounting for sources and sinks of radiation. These models have input parameters that are difficult to measure, such as the emissivity and escape fraction of ionising photons from galaxies and AGNs, and the distribution of H I absorbers (e.g. Haardt & Madau 1996; Shull et al. 1999; Faucher-Giguère et al. 2009; Haardt & Madau 2012). Therefore, different models predict values of Γ_{HI} that differ by factors of a few, primarily because the observational data that enter the modelling are not well known. As an example, the most recent models of the low-redshift UVB (Khaire & Srianand 2015; Madau & Haardt 2015; Oñorbe, Hennawi & Lukić 2017; Puchwein et al. 2018), adopting an updated AGN emissivity, predict a value of Γ_{HI} at $z \simeq 0$ which lies a factor of $\simeq 2$ above the value predicted by Haardt & Madau (2012). However, independently upon details, all recently proposed models agree with a UVB which is largely dominated by AGNs at low redshifts.

The amplitude of the UVB can be measured by three different methods. First, the hydrogen ionization rate per ion, Γ_{HI} , can be inferred using the so-called proximity effect (e.g. Murdoch et al. 1986; Bajtlik, Duncan & Ostriker 1988), i.e. by determining out to which distance the local ionization front of a single QSO outshines the UVB. Secondly, constraints on Γ_{HI} can be derived from the statistical comparison of the observed Ly α forest to numerical simulation predictions (e.g. Rauch et al. 1997; Calverley et al. 2011). This method, albeit affected by systematic uncertainties, offers the primary constraints on Γ_{HI} both at low (e.g. Khaire & Srianand 2015; Shull et al. 2015; Gaikwad et al. 2017; Viel et al. 2017, for $z \lesssim 1$) and high (e.g. Bolton et al. 2005; Kirkman et al. 2005; Faucher-Giguère et al. 2008; Wyithe & Bolton 2011; Becker & Bolton 2013; Davies et al. 2018, for $2 \lesssim z \lesssim 6$) redshifts. Note however that observing the Ly α forest at $z \lesssim 1$ requires UV spectroscopy from space.

A third method, the detection of fluorescence Ly α from the recombining IGM overdensities in ionization equilibrium with the UVB, proved to be extremely challenging because of the very low surface brightness (SB) involved (see e.g. Gould & Weinberg 1996; Cantalupo et al. 2005; Rauch et al. 2008; Gallego et al. 2018). However, fluorescence could also be detected in H α in the local Universe, hence without the redshift SB dimming effect as in the case of Ly α , by observing the ionization front in clouds photoionized by the UVB (Donahue, Aldering & Stocke 1995; Vogel et al. 1995; Weymann et al. 2001), or in the outskirts of the H I discs of galaxies (e.g. Maloney 1993; Dove & Shull 1994; Bland-Hawthorn, Freeman & Quinn 1997; Ćirković, Bland-Hawthorn & Samurović 1999; Madsen et al. 2001; Bland-Hawthorn et al. 2017). Using this technique, Adams et al. (2011) targeted the nearby edge-on galaxy UGC 7321, obtaining an upper limit for Γ_{HI} .

In a recent paper (Fumagalli et al. 2017) we described the results from a pilot MUSE (Bacon et al. 2010) observation at the VLT, following the line proposed by Adams et al. (2011), in the attempt to measure the UVB intensity by searching for the H α recombination line at the edge of the H I disc in the nearby, edge-on disc galaxy UGC 7321. We described how an emission line was detected in a deep 5.7-hr exposure at $\lambda \simeq 6574 \text{ \AA}$, which is the wavelength where H α is expected given the H I radial velocity of UGC 7321. Despite the presence of a skyline at similar wavelengths, we consistently recovered the H α signal within data cubes reduced with different pipelines, and within data cubes containing two independent sets of exposures. We concluded that we indeed detected H α recombination radiation at a level of $(1.2 \pm 0.5) \times 10^{-19} \text{ erg s}^{-1} \text{ cm}^{-2} \text{ arcsec}^{-2}$. Assuming photoionization from the UVB as origin of the observed signal, through 1D RT calculations and the joint analysis of spatially resolved H I column

density and H α SB maps, we translated the observed SB into a value for Γ_{HI} of the order of $(6 - 8) \times 10^{-14} \text{ s}^{-1}$, consistent with the values inferred from the statistics of the low-redshift Ly α forest.

In this paper we present a more refined statistical analysis of our data based on a Monte Carlo Markov's Chain (MCMC) procedure, leading to a more precise and robust determination of the UVB in terms of Γ_{HI} and its associated error.

2 DATA PRODUCTION AND ANALYSIS

A thorough discussion of our H α fluorescence line detection, with all relevant technical information, can be found in Fumagalli et al. (2017). Here we simply summarize the main key points.

The MUSE observations of the edge-on disc galaxy UGC 7321 have been acquired between 2015 June and 2016 January at the UT4 VLT, as part of the programme ID 095.A-0090 (P.I. Fumagalli). The location of the MUSE pointing was chosen to overlap with the region where the H α SB was expected to be maximized by the limb brightening according to the galaxy model presented in Adams et al. (2011), although our analysis subsequently revealed an offset.

After standard data reduction of the exposures, we applied and compared three different pipelines in order to obtain our final data cube: (i) the ESO MUSE pipeline (v1.6.2; Weilbacher et al. 2014); (ii) the CUBEXTRACTOR package (Cantalupo, in preparation), following Fumagalli et al. (2016) and Borisova et al. (2016), and (iii), a custom post-processing pipeline combined to the ZURICH ATMOSPHERE PURGE (ZAP) package (Soto et al. 2016). Moreover, to fully assess the performance of the data reduction techniques employed, we made use of mock data cubes that included emission lines injection at desired wavelengths followed by line recovery procedures.

H α recombination signal was then searched both in 2D maps and in the mean spectra constructed by averaging the flux from all the pixels inside a specified region. Further tests on the origin of the detected signal were performed. Based on this analysis we concluded that we detected an emission feature at $\lambda \sim 6574 \text{ \AA}$ consistently in two independent data reductions and in two independent sets of exposures with different instrument rotations. The emission overlaps with the location where H I is detected with $N_{\text{HI}} \gtrsim 10^{19} \text{ cm}^{-2}$. Altogether, these pieces of evidence corroborated the detection in the outskirts of UGC 7321 of an extended low SB signal consistent with H α recombination radiation of gas in photoionization equilibrium with the cosmic UVB.

3 GALAXY MODELS

In order to translate the H α signal into a value of Γ_{HI} , a model for the hydrogen disc of our target galaxy is needed. As in Fumagalli et al. (2017), and following Adams et al. (2011), we adopt a simple, double exponential disc, of the form

$$n_{\text{H}}(R, z) = n_{\text{H},0} \exp(-R/h_{\text{R}}) \exp(-|z|/h_z), \quad (1)$$

where $n_{\text{H}}(R, z)$ is the total hydrogen number density in cylindrical coordinates (R, z), $n_{\text{H},0}$ defines the central density, while h_{R} and h_z are, respectively, the radial scalelength and vertical scaleheight of the disc. The galaxy disc, inclusive of an He component at cosmic fraction, is then irradiated by an external ionizing radiation field, and the ionization and temperature structures are solved under the assumption of ionization and thermal equilibrium.

In order to ease the calculation, we solve for the vertical ionization and temperature of the disc at a fixed radial distance R assuming a two-sided plane parallel geometry, hence effectively reducing the 3D RT problem to a series of much simpler 1D calculations. The

final full structure of the gaseous disc in terms of temperature and ion fractions is thus reconstructed combining results of calculations with plane-parallel geometries at different R [details of the adopted RT scheme are described in Haardt & Madau 2012]. The ionization and thermal vertical structures are solved iteratively for an input power-law spectrum with spectral slope 1.8. Ionization equilibrium is achieved by balancing radiative recombinations with photoionization, including the formation and propagation of recombination radiation from H II, He II and He III. For the thermal structure, photoheating is balanced by free–free, collisional ionization and excitation, and recombinations from H II, He II, and He III. Our RT model makes a series of simplifying assumptions, e.g. ignoring metals and clumpiness. However, as our analysis will show, Γ_{HI} is primarily constrained by the SB at the ionization front, which does not appear to be very sensitive to the detail of the RT calculation, as shown also in Bland-Hawthorn et al. (2017).

The $\text{H}\alpha$ volume emissivity is then calculated as

$$\epsilon_{\text{H}\alpha}(R, z) = h\nu_{\text{H}\alpha}\alpha_{\text{H}\alpha}^{\text{eff}}(T)n_{\text{p}}(R, z)n_{\text{e}}(R, z), \quad (2)$$

where n_{p} and n_{e} are the proton and electron number densities, and $\alpha_{\text{H}\alpha}^{\text{eff}}$ is the $\text{H}\alpha$ effective case A (i.e. all transitions are assumed optically thin) recombination coefficient (Pequignot, Petitjean & Boisson 1991). Assuming instead case B (i.e. all transitions to the ground state are optically thick) would result in $\alpha_{\text{H}\alpha}^{\text{eff}}$ which is a factor of $\simeq 1.5$ larger for the typical temperature ($\simeq 10^4$ K) we find at the I-front (Pequignot et al. 1991). This would imply a similar *reduction* in the estimated value of Γ_{HI} . Both limiting cases are clearly a simplification of the actual physical conditions, and we may generally expect that case A and case B conditions are verified at the opposite sides of the I-front. In this respect, we estimate that our assumption of case A would lead to an overestimate $\lesssim 30$ per cent of Γ_{HI} .

The H I column density and the $\text{H}\alpha$ SB maps are then derived by integrating the neutral hydrogen density n_{HI} and $\epsilon_{\text{H}\alpha}$ along the line of sight, assuming an inclination angle of 83° (Adams et al. 2011). Details concerning the relations that connect cylindrical coordinates (R, z) to the projected position (b_1, b_2) can be found in Fumagalli et al. (2017).

We run a total of 7056 galaxy models, varying $n_{\text{H},0}$ from 0.1 to 6.0 cm^{-3} in 16 unevenly spaced intervals, the disc scalelength in the interval $h_{\text{R}} = 1.3 - 2.9 \text{ kpc}$ in nine steps of 200 pc, and the disc scaleheight in the interval $h_z = 100 - 700 \text{ pc}$ in seven steps of 100 pc. For each combination of disc parameters, we perform the RT calculation for seven different values of the UVB intensity, $\Gamma_{-14} = (1, 2, 4, 6, 8, 12, 16)$, where $\Gamma_{-14} \equiv \Gamma_{\text{HI}}/(10^{-14} \text{ s}^{-1})$.

4 RESULTS AND DISCUSSION

The inclusion of 21-cm data is instrumental in breaking the degeneracy between the $\text{H}\alpha$ SB and the hydrogen density. Indeed, if taken separately, H I and $\text{H}\alpha$ data can provide only weak constraints on Γ_{HI} . In principle, MUSE could provide spatially resolved SB maps, and one could derive tight constraints on Γ_{HI} through a joint analysis of H I and $\text{H}\alpha$ 2D maps. In practice, the large uncertainty of current line measurements makes a detailed 2D analysis unnecessary at this stage. We therefore make use of the integrated $\text{H}\alpha$ flux in MUSE field of view (FOV). Specifically, we integrated the 2D $\text{H}\alpha$ flux within the region defined by the 21-cm contour at $N_{\text{HI}} = 10^{19} \text{ cm}^{-2}$ (the reference ‘I-front’ contour), obtaining a SB of $(1.2 \pm 0.5) \times 10^{-19} \text{ erg s}^{-1} \text{ cm}^{-2} \text{ arcsec}^{-2}$. The associated error is dominated by systematics in proximity to a bright sky line at $\lambda \simeq 6577 \text{ \AA}$ and at the edges of the FOV. We require that the $\text{H}\alpha$ SB measured in models in the same area matches the observed value within the errors.

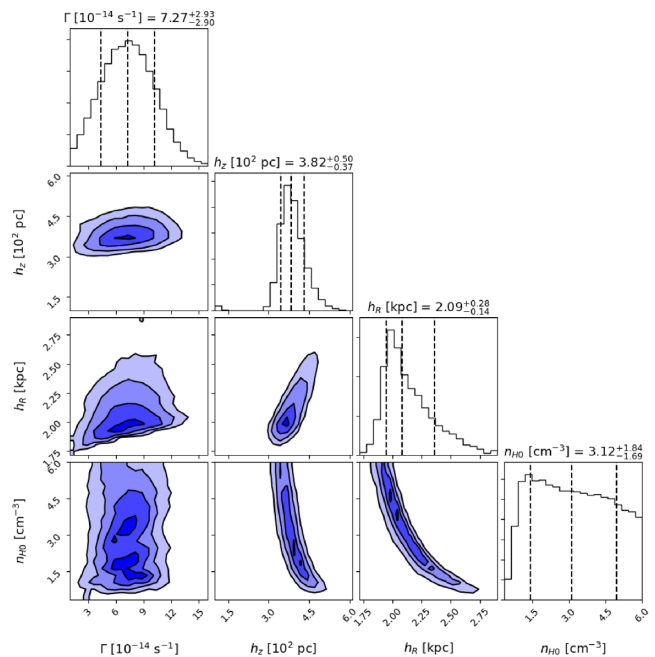


Figure 1. Corner plot from the MCMC statistical analysis of our $\text{H}\alpha$ detection plus H I contours. Systematics on the measured SB reflects into the relatively large uncertainties of the UVB estimate. However, Γ_{HI} is largely independent upon galaxy model details. Note the degeneracy of the parameters defining the galaxy gas distribution, in particular $n_{\text{H},0}$ and h_{R} .

Concerning N_{HI} data, we do not directly employ a statistical analysis of 21 cm maps. Rather, we identify three different parameters that, jointly, constrain the position of the ionization front. First, we demand that the semi-major and semi-minor axes measured in models at the I-front contour match the observed values of $b_{1,\text{HI}} = 12.4 \pm 0.1 \text{ kpc}$ and $b_{2,\text{HI}} = 2.3 \pm 0.2 \text{ kpc}$ within the associated errors. Secondly, we ask that the area in the MUSE FOV within the same contour level measured in models matches (in terms of total number of MUSE pixels) the observed value of 15000 ± 150 pixels. The associated error of 1 per cent is meant to account for an uncertainty of ± 1 pixel around the position of the I-front contour.

The posterior distributions of the four model parameters, i.e. $n_{\text{H},0}$, h_{R} , h_z and Γ_{HI} , are then derived through an MCMC analysis,¹ assuming flat priors. In order to speed-up the MCMC analysis, we construct multidimensional functions that linearly interpolate in the 4D model parameter space, rather than performing the calculation at each step. Results in terms of the so-called corner plot are shown in Fig. 1. The value $\Gamma_{-14} = 7.27^{+2.93}_{-2.90}$ is consistent with what we derive in Fumagalli et al. (2017), hence higher than the upper limit reported by Adams et al. (2011). The UVB intensity we derive is consistent with estimates of Γ_{HI} inferred from flux decrement analysis of the low-redshift ($z \lesssim 0.4$) Ly α forest in the absorption spectra of distant quasars, specifically Shull et al. (2015), Viel et al. (2017), and Gaikwad et al. (2017). The relatively large error on our UVB estimate reflects the uncertainties, mainly due to systematics, in our measurement of the $\text{H}\alpha$ SB.

Recent models of the UVB (e.g. Khaire & Srianand 2015; Madau & Haardt 2015; Oñorbe et al. 2017; Puchwein et al. 2018), adopting an updated, larger AGN emissivity at low-redshift compared to Haardt & Madau (2012), predict a value of Γ_{HI} consistent

¹We use the emcee code by Foreman-Mackey et al. (2013).

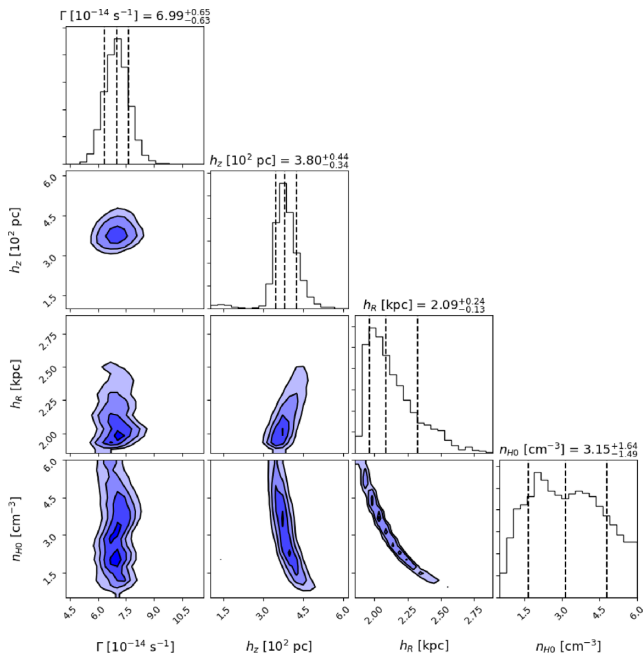


Figure 2. Same as Fig. 1, but after having artificially reduced the errors on the $H\alpha$ SB by a factor of 5.

with our estimate. In such models the UVB is largely dominated by AGNs up to $z \lesssim 2.5$, with star-forming galaxies giving a negligible contribution.

Fig. 1 shows that the central hydrogen density is degenerate with h_R and h_z , as different combinations of the three parameters result in the same density at a given position. Conversely, Γ_{HI} does not appear to be degenerate with other parameters. This means that, for observed $H\alpha$ SB and N_{HI} , Γ_{HI} is largely independent upon details on galaxy models, being primarily dependent on the SB at the ionization front.

We further checked that the uncertainties on the determination of Γ_{HI} scale approximatively with the error on the $H\alpha$ SB. By artificially reducing the error on the SB data by a factor of 2 and 5 we obtain $\Gamma_{-14} = 7.03^{+1.57}_{-1.50}$ and $6.99^{+0.65}_{-0.63}$, respectively. Errors on the other parameters are almost unchanged (see Fig. 2 for the case in which the errors on the $H\alpha$ SB are reduced by a factor of 5).

We repeated the same exercise excluding any information from 21-cm data. In this case the uncertainties on the Γ_{HI} are much less affected by any reduction of the uncertainties on the $H\alpha$ SB. As an example, the test with the error on SB data reduced by a factor of 5 leads to a corresponding reduction on the error of Γ_{HI} by less than a factor of 2. This highlights the importance of joint analysis of $H\alpha$ and 21-cm data.

5 CONCLUSIONS

Thanks to pilot MUSE observations (Fumagalli et al. 2017), we detected $H\alpha$ emission in the outskirts of the nearby edge-on spiral UGC 7321, at the spatial location, wavelength position, and intensity expected for $H\text{I}$ in ionization equilibrium with the cosmic extragalactic UVB.

By means of a large set of RT galaxy models, and MCMC statistical analysis, we translated our detection into a value of the UVB at $z \simeq 0$, which is consistent with several other independent measurements obtained with different techniques. When compared to empirical synthetic models of the UVB, our result strengthens

the notion that the low-redshift ionizing photon budget is largely dominated by AGNs, with star-forming galaxies giving a marginal contribution. This is consistent with the low fraction of ionizing photons leaking into the IGM generally measured in bright galaxies (see e.g. Kakiichi et al. 2018, and references therein). Incidentally, the decline of the AGN number density at $z \gtrsim 2$ (but see Giallongo et al. 2015) requires that such escape fraction has to be on average much larger, $\gtrsim 15$ per cent, in high-redshift galaxies if they are responsible for the reionization of the IGM at $z \gtrsim 6$ (e.g. Khaire et al. 2016). It is interesting to note that, in such picture, the declining population of AGNs and the rising escape fraction from star-forming galaxies must concur to produce an almost constant ionization rate, $\Gamma_{\text{HI}} \simeq 10^{-12} \text{ s}^{-1}$, in the redshift range $2 \lesssim z \lesssim 6$ (e.g. Becker & Bolton 2013).

Further observations are required to confirm our measurements and track with new techniques the amplitude of the UVB with redshift. Our MCMC analysis demonstrates that the derived value of Γ_{HI} is robust against large variations in the galaxy model, and that the uncertainties are mainly driven by the errors associated with the observed $H\alpha$ SB. This implies that future, deeper observations using a similar technique would be able to put much more stringent constraints on the value of the UVB. As we have shown, a reduction of the uncertainties on the measured $H\alpha$ SB would lead to a proportional reduction in the Γ_{HI} error estimate. In this respect, we anticipate that new MUSE observations of the same target (but in two different galaxy's regions) are currently scheduled at VLT (PID 101.A-0042, PI Fumagalli). These will test more robustly the origin of the detected signal and are expected to yield a more precise and accurate determination of the $H\text{I}$ photoionization rate at $z \simeq 0$.

ACKNOWLEDGEMENTS

MF acknowledges support by the Science and Technology Facilities Council (grant number ST/P000541/1). SC gratefully acknowledges support from Swiss National Science Foundation grant PP00P2_163824. This project has received funding from the European Research Council (ERC) under the European Union's Horizon 2020 research and innovation programme (grant agreement No.757535).

REFERENCES

- Adams J. J., Uson J. M., Hill G. J., MacQueen P. J., 2011, *ApJ*, 728, 107
- Bacon R. et al., 2010, Ground-based and Airborne Instrumentation for Astronomy III, Proc. of the SPIE, Vol. 7735, p. 773508
- Bajtlik S., Duncan R. C., Ostriker J. P., 1988, *ApJ*, 327, 570
- Becker G. D., Bolton J. S., 2013, *MNRAS*, 436, 1023
- Bland-Hawthorn J., Freeman K. C., Quinn P. J., 1997, *ApJ*, 490, 143
- Bland-Hawthorn J., Maloney P. R., Stephens A., Zovaro A., Popping A., 2017, *ApJ*, 849, 51
- Bolton J. S., Haehnelt M. G., 2007, *MNRAS*, 382, 325
- Bolton J. S., Haehnelt M. G., Viel M., Springel V., 2005, *MNRAS*, 357, 1178
- Borisova E. et al., 2016, *ApJ*, 831, 39
- Calverley A. P., Becker G. D., Haehnelt M. G., Bolton J. S., 2011, *MNRAS*, 412, 2543
- Cantalupo S., Porciani C., Lilly S. J., Miniati F., 2005, *ApJ*, 628, 61
- Ćirković M. M., Bland-Hawthorn J., Samurović S., 1999, *MNRAS*, 306, L15
- Davies F. B., Hennawi J. F., Eilers A.-C., Lukić Z., 2018, *ApJ*, 855, 106
- Donahue M., Aldering G., Stocke J. T., 1995, *ApJ*, 450, L45
- Dove J. B., Shull J. M., 1994, *ApJ*, 423, 196
- Faucher-Giguère C.-A., Lidz A., Hernquist L., Zaldarriaga M., 2008, *ApJ*, 682, L9

- Faucher-Giguère C.-A., Lidz A., Zaldarriaga M., Hernquist L., 2009, *ApJ*, 703, 1416
- Foreman-Mackey D., Hogg D. W., Lang D., Goodman J., 2013, *PASP*, 125, 306
- Fumagalli M., Cantalupo S., Dekel A., Morris S. L., O’Meara J. M., Prochaska J. X., Theuns T., 2016, *MNRAS*, 462, 1978
- Fumagalli M., Haardt F., Theuns T., Morris S. L., Cantalupo S., Madau P., Fossati M., 2017, *MNRAS*, 467, 4802
- Gaikwad P., Srianand R., Choudhury T. R., Khaire V., 2017, *MNRAS*, 467, 3172
- Gallego S. G. et al., 2018, *MNRAS*, 475, 3854
- Giallongo E. et al., 2015, *A&A*, 578, A83
- Gould A., Weinberg D. H., 1996, *ApJ*, 468, 462
- Gunn J. E., Peterson B. A., 1965, *ApJ*, 142, 1633
- Haardt F., Madau P., 1996, *ApJ*, 461, 20
- Haardt F., Madau P., 2012, *ApJ*, 746, 125
- Kakiichi K. et al., 2018, *MNRAS*, 479, 43
- Khaire V., Srianand R., 2015, *MNRAS*, 451, L30
- Khaire V., Srianand R., Choudhury T. R., Gaikwad P., 2016, *MNRAS*, 457, 4051
- Kirkman D. et al., 2005, *MNRAS*, 360, 1373
- Kulkarni G., Worseck G., Hennawi J. F., 2018, preprint ([arXiv:1807.09774](https://arxiv.org/abs/1807.09774))
- McDonald P. et al., 2005, *ApJ*, 635, 761
- Madau P., Haardt F., 2015, *ApJ*, 813, L8
- Madsen G. J., Reynolds R. J., Haffner L. M., Tufte S. L., Maloney P. R., 2001, *ApJ*, 560, L135
- Maloney P., 1993, *ApJ*, 414, 41
- Miralda-Escude J., Ostriker J. P., 1990, *ApJ*, 350, 1
- Murdoch H. S., Hunstead R. W., Pettini M., Blades J. C., 1986, *ApJ*, 309, 19
- Okamoto T., Gao L., Theuns T., 2008, *MNRAS*, 390, 920
- Oñorbe J., Hennawi J. F., Lukić Z., 2017, *ApJ*, 837, 106
- Pequignot D., Petitjean P., Boisson C., 1991, *A&A*, 251, 680
- Planck Collaboration et al., 2018, preprint ([arXiv:1807.06209](https://arxiv.org/abs/1807.06209))
- Puchwein E., Haardt F., Haehnelt M. G., Madau P., 2018, preprint ([arXiv:1801.04931](https://arxiv.org/abs/1801.04931))
- Rauch M. et al., 1997, *ApJ*, 489, 7
- Rauch M. et al., 2008, *ApJ*, 681, 856
- Shull J. M., Roberts D., Giroux M. L., Penton S. V., Fardal M. A., 1999, *AJ*, 118, 1450
- Shull J. M., Moloney J., Danforth C. W., Tilton E. M., 2015, *ApJ*, 811, 3
- Slosar A. et al., 2013, *J. Cosmol. Astropart. Phys.*, 4, 026
- Soto K. T., Lilly S. J., Bacon R., Richard J., Conseil S., 2016, *MNRAS*, 458, 3210
- Theuns T., Schaye J., Zaroubi S., Kim T.-S., Tzanavaris P., Carswell B., 2002, *ApJ*, 567, L103
- Viel M., Haehnelt M. G., Springel V., 2010, *J. Cosmol. Astropart. Phys.*, 6, 015
- Viel M., Haehnelt M. G., Bolton J. S., Kim T.-S., Puchwein E., Nasir F., Wakker B. P., 2017, *MNRAS*, 467, L86
- Vogel S. N., Weymann R., Rauch M., Hamilton T., 1995, *ApJ*, 441, 162
- Weilbacher P. M., Streicher O., Urrutia T., Pécontal-Rousset A., Jarno A., Bacon R., 2014, in Manset N., Forshay P., eds, ASP Conf. Ser. Vol. 485, *Astronomical Data Analysis Software and Systems XXIII*, Astron. Soc. Pac., San Francisco, p. 451
- Weymann R. J., Vogel S. N., Veilleux S., Epps H. W., 2001, *ApJ*, 561, 559
- Worseck G., Prochaska J. X., Hennawi J. F., McQuinn M., 2016, *ApJ*, 825, 144
- Wyithe J. S. B., Bolton J. S., 2011, *MNRAS*, 412, 1926

This paper has been typeset from a $\text{\TeX}/\text{\LaTeX}$ file prepared by the author.